Rare Metal Materials and Engineering
Volume 51, Issue 2, February 2022
Available online at www.rmme.ac.cn

Science Press

Cite this article as: Wang Dahui, Gan Xianhao, Chen Huaijing, et al. Estimation of Thermodynamic Properties of $Li_{1+x}M_{1-x}O_2$ Cathode Material for Lithium-Ion Battery (Lithium-Rich) Based on the Group Contribution Method[J]. Rare Metal Materials and Engineering, 2022, 51(02): 442-451.

ARTICLE

Estimation of Thermodynamic Properties of $Li_{1+x}M_{1-x}O_2$ Cathode Material for Lithium-Ion Battery (Lithium-Rich) Based on the Group Contribution Method

Wang Dahui[1], Gan Xianhao[1], Chen Huaijing[2], Yang Lixin[1], Hu Pingping[1], Liu Zhenning[1]

[1] State Key Laboratory of Advanced Processing and Recycling of Nonferrous Metals, Lanzhou University of Technology, Lanzhou 730050, China; [2] College of Science, Lanzhou University of Technology, Lanzhou 730050, China

Abstract: Given the lack of thermodynamic data on $Li_{1+x}M_{1-x}O_2$ materials, $LiAlO_2$ was split in accordance with the principle of the group contribution method. Mathematical models for estimating the $\Delta G^{\theta}_{f,298}$, $\Delta H^{\theta}_{f,298}$, and C_p of $LiAlO_2$ were proposed on the basis of thermodynamic principles. The group contribution method was used to estimate the $\Delta G^{\theta}_{f,298}$, and $\Delta H^{\theta}_{f,298}$ of 56 solid inorganic compounds and the $C_{p,298}$ of 54 solid inorganic compounds to test the reliability and applicability of the model. The group contribution method was used to estimate the mathematical model of solid inorganic compounds. Results show that the experimental data selected by fitting group parameters are accurate and reliable, and the group division method is appropriate. Mathematical models for estimating the $\Delta G^{\theta}_{f,298}$, $\Delta H^{\theta}_{f,298}$, and C_p of three types of $Li_{1+x}M_{1-x}O_2$ materials were constructed on the basis of the satisfactory results. The $\Delta G^{\theta}_{f,298}$, $\Delta H^{\theta}_{f,298}$, and $C_{p,298}$ of the 63 common $Li_{1+x}M_{1-x}O_2$ materials were also estimated.

Key words: lithium-rich cathode materials; the group contribution method; $\Delta G^{\theta}_{f,298}$; $\Delta H^{\theta}_{f,298}$; $C_{p,298}$

The gradual depletion of traditional fossil energy has led to the emergence of various energy materials and energy conversion devices. Electromagnetic (EM) functional materials support the rapid expansion of modern automation engineering, electronic science and information technology. As representatives of low-dimensional electromagnetic functional materials, silicon carbide, zinc oxide, carbon materials, transition metals and their oxides, metal-organic framework materials, etc, due to their excellent electromagnetic functions, have been used in the fields of communication and imaging, electromagnetic wave absorption and shielding, etc, showing a broad application prospect[1]. In addition, a lot of work is continuously devoted to the development and update of the collection and conversion of environmental capabilities, such as water wave energy, light energy, and heat energy[2]. High-performance rechargeable lithium-ion batteries, as a representative of advanced energy storage technology, have made great efforts to develop cathode and anode materials. For example, Cao et al prepared layered $NiCo_2O_4$ nanofibers assembled with hollow nanoparticles through simple electrospinning technology and annealing process to improve the electrochemical performance of lithium-ion batteries[3]. Cao et al[4] designed a high-capacity electrode with a three-dimensional layered Co_3O_4 flower-like structure with mesogenic nanostructures.

Lithium-ion batteries have the characteristics of light weight, small size, low self-discharge rate, long cycle life, and wide operating temperature range while lack of memory effect. Since their inception, lithium-ion batteries have been developed rapidly and widely used in 3C digital consumer electronics products, pure electric vehicles (EVs), hybrid vehicles (HEVs), and plug-in HEVs[5-7]. The challenges of lithium-ion batteries continue to grow with the increasing functional demands of consumer electronic products and the mounting of EVs. The lithium-ion battery cathode material $LiCoO_2$ and ternary material $LiNi_xCo_yMn_zO_2$ has a theoretical specific capacity of 272 mAh/g, but it is prone to irreversible

Received date: February 15, 2021
Foundation item: National Natural Science Foundation of China (51864032); Joint Fund Between Shenyang National Laboratory for Materials Science and State Key Laboratory of Advanced Processing and Recycling of Nonferrous Metals (18LHZD002)
Corresponding author: Wang Dahui, Ph. D., Professor, State Key Laboratory of Advanced Processing and Recycling of Nonferrous Metals, Lanzhou University of Technology, Lanzhou 730050, P. R. China, E-mail: wangdh@lut.edu.cn

phase change due to excessive delithiation in actual use. Generally, the maximum deintercalation of lithium accounts for 60%~80% of the total content. Thus, the actual specific capacity of the lithium-ion battery cathode material is less than 200 mAh/g, which is lower than the anode capacity of commercial carbon electrodes (350 mAh/g). In turn, the anode capacity of commercial carbon electrodes is considerably lower than that of silicon and tin anode electrodes. Given that the energy density of lithium-ion batteries depends mainly on the specific capacity of their cathode materials, researching and developing new lithium-ion battery cathode materials with increased specific capacity is necessary to meet the development requirements of EVs and HEVs in the future[8,9].

Lithium-ion battery cathode materials currently on the market are mainly classified as (1) hexagonal layered $LiCoO_2$, $LiNiO_2$, and $LiNi_xCo_yMn_2O_2$ structures with R-3m spatial point groups; (2) spinel-structured $LiMn_2O_4$ with Fd-3m spatial point groups; and (3) compound $LiFePO_4$ with a polyanionic structure. The difference in the spatial structure determines the lithium ion adsorption behavior and electrochemical performance of the two-dimensional material, and from the micro level, the basic relationship between the electronic structure and its electrochemical properties is that the electrical conductivity of the material and the adsorption strength of the intermediate are the key factors determining the electrocatalytic kinetics[10].

Lithium-rich cathode materials ($Li_{1+x}M_{1-x}O_2$, $0<x<1$, M=Ni, Co, Mn…) have an α-$NaFeO_2$ structure and belong to the hexagonal crystal system and the R-3m space group. Li occupies the 3*a* position, the transition metal *M* occupies the 3*b* position, and O occupies the 6*c* position. The transition metal layer Li, transition metal *M*, and the structure of the transition metal layer are similar to those of $LiCoO_2$[11-13]. The lithium-rich $Li_{1+x}M_{1-x}O_2$ cathode material is a solid solution that is composed of different proportions of $LiMO_2$ and Li_2MnO_3 materials, namely $xLi_2MnO_3\cdot(1-x)LiMO_2$ ($0<x<1$, M =Ni, Co, Cr, Fe, Al, Mg, Ni-Co, Ni-Mn, Ni-Co-Mn…), if the cation ordering problem is ignored. $LiMO_2$ has an α-$NaFeO_2$ layered structure and belongs to the R-3m space group. Transition metal ions occupy octahedral positions to form the MO_6 layer in $LiMO_2$; by contrast, and the structure in the Li layer is tetrahedral[14,15]. Li_2MnO_3 belongs to the monoclinal crystal system and the C2/m spatial group and is a layered rock salt structure. Li^+ and Mn^{4+} in Li_2MnO_3 are arranged alternately at the molar ratio of 1:2 to form a transition metal layer [$Li_{1/3}Mn_{2/3}$]. The superlattice structure is ascribed to the mixing effect of Li^+ and Mn^{4+} present between transition metal layers and is reflected as a sawtooth peak in the 2θ range of 20°~28° in XRD patterns. The lithium-rich cathode material is also considered as a transition metal moiety that replaces Li^+ and Mn^{4+} in the Li[Li Mn]O transition metal layer, which is expressed as $Li[M_{1-x}Li_{x/3}Mn_{2x/3}]O_2$[16,17]. The valence states of the transition metals are Ni^{2+}, Co^{3+} and Mn^{4+}, and the three elements have different effects on material electrochemical properties. Mn^{4+} can improve material structural stability, thermal stability, and safety while reducing the costs. Nevertheless, it lacks electrochemical activity during charging. Excessive Mn^{4+} content will reduce the specific capacity of materials and subsequently facilitate spinel phase production and destroy the layered material structure. Although Ni^{2+} is helpful for improving charging and discharging capacity, excessive Ni^{2+} will cause a miscible effect in combination with Li^+. This miscible effect will result in poor cycling performance and multiplier performance. Co^{3+} can effectively inhibit cationic mixing and improve electronic conductivity and cycle performance of the material. However, increasing Co^{3+} ratio will reduce capacity[18-21]. Fig.1 shows the schematic of the layered Li_2MnO_3 and $LiMO_2$ structures, where *M* is a transition metal, such as Ni, Co, or Mn.

The initial discharge specific capacity of the lithium-rich material in the high voltage state can exceed 300 mAh/g, which is much higher than that of currently commercially available cathode materials. However, layered lithium-rich materials cannot meet application requirements because they exhibit several problems, such as large initial irreversible capacity loss, voltage attenuation during cycling, low tap density, and poor rate performance[22,23]. These deficiencies can be improved through element doping and surface coating. Layered lithium-rich materials are now considered as ideal cathode materials for next-generation lithium-ion batteries with the development of the synthesis and modification technology of lithium-rich materials, because of their high specific capacity, excellent cycling ability and novel electrochemical charging and discharging mechanism[24-26].

Current research on lithium-rich $Li_{1+x}M_{1-x}O_2$ materials is mainly focused on their structure and electrochemical properties and little attention is paid on their thermodynamic properties. The development of novel lithium-rich $Li_{1+x}M_{1-x}O_2$ materials with high energy density and capacity is dependent on the internal relationship among their structures, thermodynamic properties, and electrochemical properties. It is specifically manifested with changing the crystal phase of the material by adjusting the different charge distribution and electronic structure of various atomic configurations. The phase change process in the chemical reaction involved in this process requires reliable thermodynamic data to guide. It also provides a theoretical reference for estimating actual battery energy density and theoretical capacity. Other issues include the further improvement of the charging and discharging performances of lithium-ion batteries, the development of new

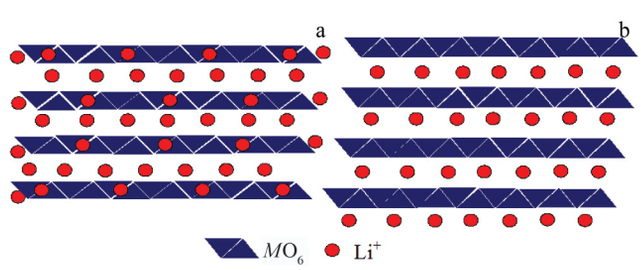

Fig.1 Structural schematic diagram of layered Li_2MnO_3 (a) and $LiMO_2$ (b) (*M* is Ni, Co, or Mn)

electrode materials and battery systems, and the optimization of battery structure. The limited understanding of the thermodynamic properties of $Li_{1+x}M_{1-x}O_2$ restricts the development and utilization of new lithium-rich materials. The study of the thermodynamic properties of $Li_{1+x}M_{1-x}O_2$ are crucial for guiding theoretical calculations toward the improvement and usage of lithium-rich new materials in the long run.

Mostafa et al[27,28] proposed that the thermodynamic properties of solid inorganic compounds are the sum of the thermodynamic group contributions of their constituent cations, anions, and ligands (such as water of crystallization). The $\Delta H^{\theta}_{f,298}$ values of 938 solid inorganic compounds and the $\Delta G^{\theta}_{f,298}$ values of 687 solid inorganic compounds were subjected to multiple linear regression analysis (84% of the data are published by the International Union of Pure and Applied Chemistry). The group contribution values of 136 cations, 23 anions, and 5 ligand molecules were obtained, and the relative errors of each group contribution value were estimated by the standard deviation of the parameters. The $C_{p,298}$ values of 664 solid inorganic compounds were also subjected to multiple linear regression analysis. The group contribution values of 129 cations, 17 anions, and 2 ligands were acquired. The group contribution method has a wide range of applications and high reliability and accuracy. Thus, the mathematical models for estimating the $\Delta H^{\theta}_{f,298}$, $\Delta G^{\theta}_{f,298}$, and C_p of three kinds of lithium-rich $Li_{1+x}M_{1-x}O_2$ materials were constructed for the first time by the group contribution method. Moreover, the $\Delta H^{\theta}_{f,298}$, $\Delta G^{\theta}_{f,298}$ and $C_{p,298}$ of 63 common lithium-rich $Li_{1+x}M_{1-x}O_2$ materials were estimated.

1 Estimation Method

1.1 Mathematical model for estimating the thermodynamic data of matter using the group contribution method

The success of the group contribution method in estimating material property data is associated with the physical basis of the mathematical model related to group parameters and properties, the accuracy and reliability of the experimental data selected for fitting group parameters, and the appropriateness of the group partitioning method. $LiAlO_2$ was split in accordance with the principle of the said method to determine the reliability and application range of the group contribution method for estimating the $\Delta H^{\theta}_{f,298}$, $\Delta G^{\theta}_{f,298}$ and $C_{p,298}$ of solid inorganic compounds. Moreover, the mathematical models for estimating the $\Delta H^{\theta}_{f,298}$, $\Delta G^{\theta}_{f,298}$ and C_p of $LiAlO_2$ were proposed in accordance with thermodynamic principles.

Table 1 shows the group contribution values of Li^+, Ni^{2+}, Ni^{3+}, Co^{2+}, Co^{3+}, Mn^{3+}, Mn^{4+}, and O^{2-} to the $\Delta H^{\theta}_{f,298}$ and $\Delta G^{\theta}_{f,298}$ of the solid inorganic compounds. The $\Delta H^{\theta}_{f,298}$ and $\Delta G^{\theta}_{f,298}$ of $LiAlO_2$ were estimated by the group contribution method, as follows. (1) The molecular formula of the solid inorganic compound was written. (2) The molecular formula was deconstructed into the structural groups of cations, anions, or ligands. The contribution value of each molecular structure group was multiplied by the distribution number of the group in the molecular formula. Then, the contribution value of each group was calculated. (3) The mathematical model for estimating the thermodynamic properties of the substance was established. Table 2 presents the estimation process and results.

The mathematical models for estimating the $\Delta H^{\theta}_{f,298}$ and $\Delta G^{\theta}_{f,298}$ of $LiAlO_2$ by the group contribution method are as follows:

$$\Delta H^{\theta}_{f,298}(LiAlO_2)=\Delta H^{\theta}_{f,298}(Li^+)+\Delta H^{\theta}_{f,298}(Al^{3+})+2\Delta H^{\theta}_{f,298}(O^{2-}) \quad (1)$$

$$\Delta G^{\theta}_{f,298}(LiAlO_2)=\Delta G^{\theta}_{f,298}(Li^+)+\Delta G^{\theta}_{f,298}(Al^{3+})+2\Delta G^{\theta}_{f,298}(O^{2-}) \quad (2)$$

in which 1, 1, and 2 are the distribution numbers of Li^+, Al^{3+}, and O^{2-} in the $LiAlO_2$ molecular formula, respectively.

Table 2 shows that the estimated values of the $\Delta H^{\theta}_{f,298}$, and $\Delta G^{\theta}_{f,298}$ of $LiAlO_2$ are −1193.37 and −1129.95 kJ·mol^{-1}, respectively. Compared with the values given in the literature (−1188.70 and −1126.30 kJ·mol^{-1}), it reveals that the corresponding relative errors of the estimated values are 0.39% and 0.32%[29].

Table 3 shows the group contribution values of Li^+, Ni^{2+}, Ni^{3+}, Co^{2+}, Co^{3+}, Mn^{3+}, Mn^{4+}, and O^{2-} to the C_p of the solid inorganic compound. The group contribution method was used to estimate the C_p of $LiAlO_2$, as follows. (1) The molecular formula of the solid inorganic compound was written. (2) The formula was broken into the cationic and anionic structural groups given in Table 1, and the contribution value of each group was multiplied by the distribution number of the group in the molecular formula to calculate the contribution value of each group. (3) The contribution values of $\sum_j n_j\Delta_{a,j}$, $\sum_j n_j\Delta_{b,j}$, $\sum_j n_j\Delta_{c,j}$ and $\sum_j n_j\Delta_{d,j}$ were determined by tallying the contribution values of each group. (4) The mathematical model for estimating the thermodynamic properties of the material was developed. Table 4 presents the estimation process and results.

$$\begin{aligned}C_p(LiAlO_2)&=\sum_j n_j\Delta_{a,j}+(\sum_j n_j\Delta_{b,j}\times10^{-3})T+(\sum_j n_j\Delta_{c,j}\times10^{6})/T^2\\&\quad+(\sum_j n_j\Delta_{d,j}\times10^{-6})T^2\\\sum_j n_j\Delta_{a,j}&=\Delta_{a,j}(Li^+)+\Delta_{a,j}(Al^{3+})+2\Delta_{a,j}(O^{2-})\\\sum_j n_j\Delta_{b,j}&=\Delta_{b,j}(Li^+)+\Delta_{b,j}(Al^{3+})+2\Delta_{b,j}(O^{2-})\\\sum_j n_j\Delta_{c,j}&=\Delta_{c,j}(Li^+)+\Delta_{c,j}(Al^{3+})+2\Delta_{c,j}(O^{2-})\\\sum_j n_j\Delta_{d,j}&=\Delta_{d,j}(Li^+)+\Delta_{d,j}(Al^{3+})+2\Delta_{d,j}(O^{2-})\end{aligned} \quad (3)$$

in which 1, 1, and 2 are the distribution numbers of Li^+, Al^{3+}, and O^{2-} in the $LiAlO_2$ molecular formula, respectively.

The $C_{p,298}$ of $LiAlO_2$ was calculated in accordance with the required temperature (with T=298 K as the reference data). The estimated value of $C_{p,298}$ is 67.75 J·mol^{-1}·K^{-1}. Compared with the value of 67.78 J·mol^{-1}·K^{-1} given in the literature, the relative error of the estimated value is 0.04%.

Kopp's rule states that the constant pressure heat capacity C^{θ}_p of a compound is approximately equal to the sum of the molar heat capacity of the atoms that constitute the elements of the compound, as shown in Eq. (4). Table 5 lists the contribution values of elements, such as Ca, Al, Li, Ni, Co, Mn, and O[30].

$$C^{\theta}_p=\sum_j n_j C^{\theta}_{p,j} \quad (4)$$

Table 1 Solid inorganic compound groups of cationic, anionic and ligand molecule groups, their contributions ($\Delta_{H,j}$, $\Delta_{G,j}$), number of occurrences in the regression, and standard deviations ($S_{\Delta j}$) associated with them for standard heats and free energies of formation[27]

	Group	No. of occurrence for $\Delta_{H,j}$	$\Delta_{H,j}$/kJ·mol^{-1}	$S_{\Delta j}$ for $\Delta_{H,j}$	No. of occurrence for $\Delta_{G,j}$	$\Delta_{G,j}$/kJ·mol^{-1}	$S_{\Delta j}$ for $\Delta_{G,j}$
Cation	Al^{3+}	129	−553.115	12.713	118	−420.023	23.951
	B^{3+}	50	−392.895	13.015	49	−273.681	24.327
	Be^{2+}	23	−402.267	13.713	15	−297.827	19.827
	Ca^{2+}	131	−520.898	14.734	124	−432.414	16.222
	Co^{2+}	23	−76.275	30.537	3	4.128	35.818
	Co^{3+}	1	−37.950	-	1	94.826	-
	Cr^{3+}	15	−290.075	27.492	15	−168.532	25.868
	Fe^{2+}	40	−126.475	13.177	22	−43.568	19.883
	Fe^{3+}	30	−122.815	14.811	22	−8.638	25.237
	Hf^{4+}	1	−769.852	-	1	−606.500	-
	Li^{+}	42	−292.950	8.187	29	−250.254	11.449
	Mg^{2+}	116	−461.804	9.478	72	−372.414	16.624
	Mn^{2+}	16	−250.029	14.052	13	−167.203	19.858
	Mn^{3+}	1	−167.921	-	1	−100.187	-
	Mn^{4+}	1	−85.813	-	1	66.580	-
	Mo^{6+}	38	−234.996	25.436	82	−17.811	47.790
	NH_4^{+}	8	−164.486	16.381	5	−53.199	20.031
	Ni^{2+}	20	−91.381	14.364	14	0.357	20.625
	Ni^{3+}	2	−20.042	31.141	1	149.483	-
	P^{5+}	4	−481.148	29.622	4	−285.069	44.693
	Si^{4+}	174	−575.556	16.706	159	−411.036	32.072
	Ti^{4+}	15	−571.358	22.030	17	−408.836	34.023
	V^{5+}	32	−369.937	22.053	33	−162.620	40.397
	W^{6+}	40	−367.612	26.321	40	−131.422	48.219
	Zn^{2+}	33	−191.646	11.753	32	−91.944	17.855
Anion	CO_3^{2-}	26	−616.496	14.214	28	−635.990	19.167
	F^{-}	291	−310.918	4.638	168	−326.667	8.264
	NO_3^{-}	97	−175.710	6.206	40	−126.405	10.288
	O^{2-}	1946	−173.650	8.264	1725	−229.836	15.876
	PO_4^{3-}	22	−1197.521	16.826	20	−1206.614	26.773
	SO_4^{2-}	121	−814.755	9.861	91	−795.046	16.975
Ligand molecule	H_2O	718	−298.933	1.133	394	−244.317	1.470

Table 2 Estimation of the $\Delta H^{\theta}_{f,298}$, and $\Delta G^{\theta}_{f,298}$ of $LiAlO_2$ (kJ·mol^{-1})

Group	$\Delta H^{\theta}_{f,298}$	$\Delta G^{\theta}_{f,298}$
Li^{+}	−292.50	−250.254
Al^{3+}	−553.115	−420.023
$2O^{2-}$	2×(−173.650)	2×(−229.836)
Total	−1193.37	−1129.95

The $C_{p,298}$ of $LiAlO_2$ was estimated by Kopp's rule through the following steps. (1) The molecular structure formula of the solid inorganic compound was written. (2) The molecular structure formula was broken down in accordance with the types of elements, and the contribution values of the elements were ascertained from Table 5. The contribution value of the element was multiplied by the distribution number of the component in the molecular structure equation, and the contribution value of each element was calculated. (3) The estimated and reported values of $C_{p,298}$ are 68.16 and 67.78 J·mol^{-1}·K^{-1}, respectively. Thus, the relative error of the estimated value is 0.56%. Table 6 presents the estimation process and results.

1.2 Verification of the model

The group contribution method was used to estimate the $\Delta H^{\theta}_{f,298}$ and $\Delta G^{\theta}_{f,298}$ of 56 solid inorganic compounds to determine the reliability and applicability of the model. The

Table 3 Solid inorganic salt groups of cationic, anionic groups and their contribution ($\Delta_{a,j}$, $\Delta_{b,j}$, $\Delta_{c,j}$, $\Delta_{d,j}$) and number of occurrences in the regression[28]

	Group	No. of occurrence	$\Delta_{a,j}$	$\Delta_{b,j}$	$\Delta_{c,j}$	$\Delta_{d,j}$
Cation	Al^{3+}	81	10.306	4.518	−0.623	−3.701
	B^{3+}	59	−13.188	16.765	0.273	−0.219
	Be^{2+}	16	−5.164	22.314	−0.002	6.544
	Ca^{2+}	64	20.470	−6.225	−0.026	−3.219
	Co^{2+}	17	26.552	−19.272	0.327	5.245
	Co^{3+}	1	34.158	−42.075	−0.149	−4.614
	Cr^{3+}	22	21.086	−16.392	0.067	5.298
	Fe^{2+}	15	20.486	−5.415	0.055	5.393
	Fe^{3+}	26	16.618	3.328	0.082	5.002
	Hf^{4+}	9	20.580	−22.025	−0.050	2.633
	Li^{+}	47	15.639	4.124	−0.007	7.973
	Mg^{2+}	32	14.639	−0.637	−0.074	−0.609
	Mn^{2+}	15	21.419	−15.908	0.265	5.652
	Mn^{3+}	4	8.913	3.070	0.454	5.448
	Mn^{4+}	1	−3.593	22.048	0.643	5.244
	Mo^{6+}	11	−7.473	−7.423	1.279	13.430
	Ni^{2+}	14	22.497	−6.671	−0.022	6.234
	Ni^{3+}	1	3.549	−7.964	0.413	7.913
	P^{5+}	12	−39.486	50.248	1.686	2.325
	Si^{4+}	79	−2.308	4.382	−0.041	−3.301
	Ti^{4+}	34	10.043	−7.562	0.299	11.414
	V^{5+}	20	−1.279	−5.243	0.697	13.608
	W^{6+}	20	−23.788	35.451	1.836	9.893
	Zn^{2+}	18	12.599	−0.744	0.377	4.203
	Zr^{4+}	13	17.188	−23.478	−0.063	7.098
Anion	CO_3^{2-}	15	47.278	86.757	−0.887	−5.133
	F^{-}	247	22.041	15.652	−0.244	1.538
	NO_3^{-}	120	49.766	83.928	−0.478	−7.040
	O^{2-}	1155	28.152	12.043	−0.747	−4.023
	PO_4^{3-}	6	95.827	56.863	−2.462	−7.691
	SO_4^{2-}	49	85.866	52.357	−1.925	−0.047

Table 4 Estimation of $C_{p,298}$ for $LiAlO_2$

Group	$\Delta_{a,j}$	$\Delta_{b,j}$	$\Delta_{c,j}$	$\Delta_{d,j}$
Li^{+}	15.639	4.124	−0.007	7.973
Al^{3+}	10.306	4.518	−0.623	−3.701
$2O^{2-}$	2×28.152	2×12.043	2×(−0.747)	2×(−4.023)
$\sum_j n_j\Delta_{i,j}$	82.249	32.728	−2.124	−3.774

$C_{p,298}=\sum_j n_j\Delta_{a,j}+(\sum_j n_j\Delta_{b,j}\times10^{-3})T+(\sum_j n_j\Delta_{c,j}\times10^{6})/T^2+(\sum_j n_j\Delta_{d,j}\times10^{-6})T^2$
$=82.249+(32.728\times10^{-3}\times298+(-2.124\times10^{6})/298^2$
$+(-3.774\times10^{-6}\times298^2)=67.75\ J\cdot mol^{-1}\cdot K^{-1}$

estimated and reported values of $\Delta H^{\theta}_{f,298}$ were compared[31]. The absolute values of relative errors were within 4%, and the absolute values of the relative errors of 43 kinds of solid inorganic compounds were less than 2%. The estimated and reported values of $\Delta G^{\theta}_{f,298}$ were also compared. The absolute values of relative errors were within 4%, the absolute values of the relative errors of 42 kinds of solid inorganic compounds were less than 2%. The $C_{p,298}$ values of 54 solid inorganic compounds were likewise estimated[32]. The absolute values of the relative errors of $C_{p,298}$ were within 5% of the values in the literature. The absolute values of the relative errors of 43 kinds of solid inorganic compounds were less than 2%. The $C_{p,298}$ values of 54 selected solid inorganic compounds were estimated in accordance with Kopp's rule. The absolute values of relative errors of $C_{p,298}$ were within 11% of those reported in the literature, and the absolute values of the relative errors of 33 solid inorganic compounds were less than 3%. Among them, the absolute values of the relative errors of 12 kinds of solid inorganic compounds were 3%~5%. This method has a better calculation effect than Kopp's rule estimation. The results show that the mathematical model of the correlation between group parameters and physical properties is correct, the experimental data selected by fitting the group parameters are accurate and reliable, and the group division method is appropriate.

2 Results and Discussion

Three main types of lithium-rich cathode materials are currently available: (1) lithium-rich layered $x\mathrm{Li_2MnO_3}\cdot(1-x)\mathrm{Li}M\mathrm{O_2}$ ($0<x<1$, M=Ni, Co, Cr, Fe, Al, Mg, Ni-Co, Ni-Mn, Ni-Co-Mn…) cathode material; (2) lithium-rich manganese-based $x\mathrm{Li[Li_{1/3}Mn_{2/3}]O_2}\cdot(1-x)\mathrm{Li}M\mathrm{O_2}$ ($0<x<1$, M= Ni, Co, Cr, Fe, Al, Mg, Ni-Co, Ni-Mn, Ni-Co-Mn…) solid solution material; (3) layered spinel $x\mathrm{Li[Li_{1/3}Mn_{2/3}]O_2}\cdot(1-x)\mathrm{LiMn_2O_4}$ ($0<x<1$) composite solid solution material and layered spinel $x\mathrm{Li[Li_{1/3}Mn_{2/3}]O_2}\cdot(1-x)\mathrm{LiNi_{0.5}Mn_{1.5}O_4}$ ($0<x<1$) composite solid solution material. The mathematical models for estimating $\Delta H^{\theta}_{f,298}$, and $\Delta G^{\theta}_{f,298}$, and C_p of three types of lithium-rich materials were constructed in accordance with the satisfactory results, and the $\Delta H^{\theta}_{f,298}$, and $\Delta G^{\theta}_{f,298}$ and $C_{p,298}$ of the common 63 lithium-rich materials were estimated.

2.1 Mathematical models for estimating $\Delta H^{\theta}_{f,298}$, $\Delta G^{\theta}_{f,298}$, and C_p of the lithium-rich layered $x\mathrm{Li_2MnO_3}\cdot(1-x)\mathrm{Li}M\mathrm{O_2}$ cathode materials

The chemical valences of Li, O, Mn, and M in the lithium-rich layered $x\mathrm{Li_2MnO_3}\cdot(1-x)\mathrm{LiMO_2}$ ($0<x<1$, M=Ni, Co, Cr, Fe, Al, Mg, Ni-Co, Ni-Mn, Ni-Co-Mn…) materials are +1, −2, +4, and +3, respectively. The most studied systems of the lithium-rich $x\mathrm{Li_2MnO_3}\cdot(1\text{-}x)\mathrm{LiMO_2}$ material are M=Co, Fe, and Ni-Mn. Common lithium-rich layered materials include $x\mathrm{Li_2MnO_3}\cdot(1-x)\mathrm{LiCoO_2}$, $x\mathrm{Li_2MnO_3}\cdot(1-x)\mathrm{LiFeO_2}$, and $x\mathrm{Li_2MnO_3}\cdot(1-x)\mathrm{Li[Ni_{0.5}Mn_{0.5}]O_2}$. The mathematical models for estimating $\Delta H^{\theta}_{f,298}$, $\Delta G^{\theta}_{f,298}$, and C_p of lithium-rich layered $x\mathrm{Li_2MnO_3}\cdot(1\text{-}x)\mathrm{LiMO_2}$ materials using the group contribution method are shown Eq.(5~7), respectively:

$$\Delta H^{\theta}_{f,298}(x\mathrm{Li_2MnO_3}\cdot(1-x)\mathrm{Li}M\mathrm{O_2})=2x\Delta H^{\theta}_{f,298}(\mathrm{Li^+})+x\Delta H^{\theta}_{f,298}(\mathrm{Mn^{4+}})+3x\Delta H^{\theta}_{f,298}(\mathrm{O^{2-}})+(1-x)\Delta H^{\theta}_{f,298}(\mathrm{Li^+})+(1-x)\Delta H^{\theta}_{f,298}(M^{3+})+2(1-x)\Delta H^{\theta}_{f,298}(\mathrm{O^{2-}}) \quad (5)$$

Table 5 Contribution of elements to solid inorganic compound $C_{p,298}$

Element	New Kopp's Solids	Element	New Kopp's Solids	Element	New Kopp's Solids	Element	New Kopp's Solids	Element	New Kopp's Solids
H	7.56	F	20.92	K	28.78	Ni	25.46	Ba	32.37
Li	23.25	Na	26.19	Ca	28.25	Cu	26.92	W	30.87
Be	12.47	Mg	22.69	Ti	27.24	Br	25.36	Hg	27.87
B	10.10	Al	18.07	V	29.36	Sr	28.41	Pb	31.60
C	10.89	Si	17.00	Mn	28.06	Zr	26.82	P	22.61
N	18.74	S	12.36	Fe	29.08	Mo	29.44	Cr	31.42
O	13.42	Cl	24.69	Co	25.71	I	25.29	Misc	26.63

Table 6 Estimation of $C_{p,298}$ for $LiAlO_2$

Step	$LiAlO_2$					
1	Element	$\Delta_{a,j}$	Element	$\Delta_{b,j}$	Element	$\Delta_{c,j}$
2	Li	23.25	Al	18.07	O	2×13.42
3	$\sum_j n_j\Delta_{i,j}$		68.16 J·mol^{-1}·K^{-1}			

$$\Delta G^{\theta}_{f,298}(x\mathrm{Li_2MnO_3}\cdot(1-x)\mathrm{Li}M\mathrm{O_2})=2x\Delta G^{\theta}_{f,298}(\mathrm{Li^+})+x\Delta G^{\theta}_{f,298}(\mathrm{Mn^{4+}})+3x\Delta G^{\theta}_{f,298}(\mathrm{O^{2-}})+(1-x)\Delta G^{\theta}_{f,298}(\mathrm{Li^+})+(1-x)\Delta G^{\theta}_{f,298}(M^{3+})+2(1-x)\Delta G^{\theta}_{f,298}(\mathrm{O^{2-}}) \quad (6)$$

$$\begin{aligned}C_p(x\mathrm{Li_2MnO_3}\cdot(1-x)\mathrm{Li}M\mathrm{O_2})&=\sum_j n_j\Delta_{a,j}+(\sum_j n_j\Delta_{b,j}\times10^{-3})T+(\sum_j n_j\Delta_{c,j}\times10^{6})/T^2+(\sum_j n_j\Delta_{d,j}\times10^{-6})T^2\\&=\sum_j n_j\Delta_{a,j}\\&=2x\Delta_{a,j}(\mathrm{Li^+})+x\Delta_{a,j}(\mathrm{Mn^{4+}})+3x\Delta_{a,j}(\mathrm{O^{2-}})+(1-x)\Delta_{a,j}(\mathrm{Li^+})+(1-x)\Delta_{a,j}(M^{3+})+2(1-x)\Delta_{a,j}(\mathrm{O^{2-}})\\&=\sum_j n_j\Delta_{b,j}\\&=2x\Delta_{b,j}(\mathrm{Li^+})+x\Delta_{b,j}(\mathrm{Mn^{4+}})+3x\Delta_{b,j}(\mathrm{O^{2-}})+(1-x)\Delta_{b,j}(\mathrm{Li^+})+(1-x)\Delta_{b,j}(M^{3+})+2(1-x)\Delta_{b,j}(\mathrm{O^{2-}})\\&=\sum_j n_j\Delta_{c,j}\\&=2x\Delta_{c,j}(\mathrm{Li^+})+x\Delta_{c,j}(\mathrm{Mn^{4+}})+3x\Delta_{c,j}(\mathrm{O^{2-}})+(1-x)\Delta_{c,j}(\mathrm{Li^+})+(1-x)\Delta_{c,j}(M^{3+})+2(1-x)\Delta_{c,j}(\mathrm{O^{2-}})\\&=\sum_j n_j\Delta_{d,j}\\&=2x\Delta_{d,j}(\mathrm{Li^+})+x\Delta_{d,j}(\mathrm{Mn^{4+}})+3x\Delta_{d,j}(\mathrm{O^{2-}})+(1-x)\Delta_{d,j}(\mathrm{Li^+})+(1-x)\Delta_{d,j}(M^{3+})+2(1-x)\Delta_{d,j}(\mathrm{O^{2-}})\end{aligned} \quad (7)$$

When M is Co, the mathematical models for estimating the $\Delta H^{\theta}_{f,298}$, $\Delta G^{\theta}_{f,298}$, and C_p of lithium-rich layered $x\mathrm{Li_2MnO_3}\cdot(1-x)\mathrm{Li}M\mathrm{O_2}$ materials using the group contribution method are shown in Eq.(8~10), respectively:

$$\Delta H^{\theta}_{f,298}(x\mathrm{Li_2MnO_3}\cdot(1-x)\mathrm{LiCoO_2})=-514.463x-678.200 \quad (8)$$

$$\Delta G^{\theta}_{f,298}(x\mathrm{Li_2MnO_3}\cdot(1-x)\mathrm{LiCoO_2})=-508.336x-615.100 \quad (9)$$

$$C_p(x\mathrm{Li_2MnO_3}\cdot(1-x)\mathrm{LiCoO_2})=6.040x+106.101+(80.290x-13.865)\times10^{-3}T+(0.038x-1.650)\times10^{6}/T^2+(13.808x-4.687)\times10^{-6}T^2 \quad (10)$$

When M is Fe, the mathematical models for estimating the $\Delta H^{\theta}_{f,298}$, $\Delta G^{\theta}_{f,298}$, and C_p of lithium-rich layered $x\mathrm{Li_2MnO_3}\cdot(1\text{-}x)\mathrm{Li}M\mathrm{O_2}$ materials using the group contribution method are shown in Eq.(11~13), respectively:

$$\Delta H^{\theta}_{f,298}(x\mathrm{Li_2MnO_3}\cdot(1-x)\mathrm{LiFeO_2})=-429.598x-763.065 \quad (11)$$

$$\Delta G^{\theta}_{f,298}(x\mathrm{Li_2MnO_3}\cdot(1-x)\mathrm{LiFeO_2})=-404.872x-718.564 \quad (12)$$

$$C_p(x\mathrm{Li_2MnO_3}\cdot(1-x)\mathrm{LiFeO_2})=23.580x+88.561+(34.887x+31.538)\times10^{-3}T+(-0.193x-1.419)\times10^{6}/T^2+(4.192x+4.929)\times10^{-6}T^2 \quad (13)$$

When M is $\mathrm{Ni_{1/2}Mn_{1/2}}$, the mathematical models for estimating the $\Delta H^{\theta}_{f,298}$, $\Delta G^{\theta}_{f,298}$, and C_p of lithium-rich layered $x\mathrm{Li_2MnO_3}\cdot(1-x)\mathrm{Li}M\mathrm{O_2}$ materials using the group contribution method are shown in Eq.(14~16), respectively:

$$\Delta H^{\theta}_{f,298}(x\mathrm{Li_2MnO_3}\cdot(1-x)\mathrm{LiNi_{1/2}Mn_{1/2}O_2})=-463.816x-728.847 \quad (14)$$

$$\Delta G^{\theta}_{f,298}(x\mathrm{Li_2MnO_3}\cdot(1-x)\mathrm{LiNi_{1/2}Mn_{1/2}O_2})=-446.979x-676.458 \quad (15)$$

$$C_p(x\mathrm{Li_2MnO_3}\cdot(1-x)\mathrm{LiNi_{1/2}Mn_{1/2}O_2})=30.746x+81.395+(30.527x+35.899)(10^{-3})T+(-0.422x-1.191)(10^{6})/T^2+(3.455x+5.666)(10^{-6})T^2 \quad (16)$$

2.2 Mathematical models for estimating $\Delta H^{\theta}_{f,298}$, and $\Delta G^{\theta}_{f,298}$, and C_p of lithium-rich manganese-based $x\mathrm{Li[Li_{1/3}Mn_{2/3}]O_2}\cdot(1-x)\mathrm{Li}M\mathrm{O_2}$ solid solution materials

The chemical valences of Li, O, Mn, and M in the lithium-rich manganese-based solid solution materials of $x\mathrm{Li[Li_{1/3}Mn_{2/3}]O_2}\cdot(1-x)\mathrm{Li}M\mathrm{O_2}$ (0<x<1, M=Ni, Co, Cr, Fe, Al, Mg, Ni-Co, Ni-Mn, Ni-Co-Mn…) are +1, −2, +4, and +3, respectively. The most studied systems of the lithium-rich manganese-based $x\mathrm{Li[Li_{1/3}Mn_{2/3}]O_2}\cdot(1-x)\mathrm{Li}M\mathrm{O_2}$ material are Ni-Mn, Ni-Co-Mn. Common layered lithium-rich materials include $x\mathrm{Li[Li_{1/3}Mn_{2/3}]O_2}\cdot(1-x)\mathrm{LiNi_{1/3}Co_{1/3}Mn_{1/3}O_2}$ and $x\mathrm{Li[Li_{1/3}Mn_{2/3}]O_2}\cdot(1-x)\mathrm{LiNi_{1/3}Co_{1/3}Mn_{1/3}O_2}$.

The mathematical models for estimating the $\Delta H^{\theta}_{f,298}$, $\Delta G^{\theta}_{f,298}$, and C_p of lithium-rich manganese-based $x\mathrm{Li[Li_{1/3}Mn_{2/3}]O_2}\cdot(1-x)\mathrm{Li}M\mathrm{O_2}$ (0<x<1, M=Ni, Co, Cr, Fe, Al, Mg, Ni-Co, Ni-Mn, Ni-Co-Mn…) solid solution materials by the group contribution method are shown in Eq.(17~19):

$$\Delta H^{\theta}_{f,298}(x\mathrm{Li[Li_{1/3}Mn_{2/3}]O_2}\cdot(1-x)\mathrm{Li}M\mathrm{O_2})=4/3x\Delta H^{\theta}_{f,298}(\mathrm{Li^+})+2/3x\Delta H^{\theta}_{f,298}(\mathrm{Mn^{4+}})+2x\Delta H^{\theta}_{f,298}(\mathrm{O^{2-}})+(1-x)\Delta H^{\theta}_{f,298}(\mathrm{Li^+})+(1-x)\Delta H^{\theta}_{f,298}(M^{3+})+2(1-x)\Delta H^{\theta}_{f,298}(\mathrm{O^{2-}}) \quad (17)$$

$$\Delta G^{\theta}_{f,298}(x\mathrm{Li[Li_{1/3}Mn_{2/3}]O_2}\cdot(1-x)\mathrm{Li}M\mathrm{O_2})=4/3x\Delta G^{\theta}_{f,298}(\mathrm{Li^+})+2/3x\Delta G^{\theta}_{f,298}(\mathrm{Mn^{4+}})+2x\Delta G^{\theta}_{f,298}(\mathrm{O^{2-}})+(1-x)\Delta G^{\theta}_{f,298}(\mathrm{Li^+})+(1-x)\Delta G^{\theta}_{f,298}(M^{3+})+2(1-x)\Delta G^{\theta}_{f,298}(\mathrm{O^{2-}}) \quad (18)$$

$$\begin{aligned}C_p(x\mathrm{Li[Li_{1/3}Mn_{2/3}]O_2}\cdot(1-x)\mathrm{Li}M\mathrm{O_2})&=\sum_j n_j\Delta_{a,j}+(\sum_j n_j\Delta_{b,j}\times10^{-3})T+(\sum_j n_j\Delta_{c,j}\times10^{6})/T^2+(\sum_j n_j\Delta_{d,j}\times10^{-6})T^2\\\sum_j n_j\Delta_{a,j}&=4/3x\Delta_{a,j}(\mathrm{Li^+})+2/3x\Delta_{a,j}(\mathrm{Mn^{4+}})+2x\Delta_{a,j}(\mathrm{O^{2-}})+(1-x)\Delta_{a,j}(\mathrm{Li^+})+(1-x)\Delta_{a,j}(M^{3+})+2(1-x)\Delta_{a,j}(\mathrm{O^{2-}})\\\sum_j n_j\Delta_{b,j}&=4/3x\Delta_{b,j}(\mathrm{Li^+})+2/3x\Delta_{b,j}(\mathrm{Mn^{4+}})+2x\Delta_{b,j}(\mathrm{O^{2-}})+(1-x)\Delta_{b,j}(\mathrm{Li^+})+(1-x)\Delta_{b,j}(M^{3+})+2(1-x)\Delta_{b,j}(\mathrm{O^{2-}})\\\sum_j n_j\Delta_{c,j}&=4/3x\Delta_{c,j}(\mathrm{Li^+})+2/3x\Delta_{c,j}(\mathrm{Mn^{4+}})+2x\Delta_{c,j}(\mathrm{O^{2-}})+(1-x)\Delta_{c,j}(\mathrm{Li^+})+(1-x)\Delta_{c,j}(M^{3+})+2(1-x)\Delta_{c,j}(\mathrm{O^{2-}})\\\sum_j n_j\Delta_{d,j}&=4/3x\Delta_{d,j}(\mathrm{Li^+})+2/3x\Delta_{d,j}(\mathrm{Mn^{4+}})+2x\Delta_{d,j}(\mathrm{O^{2-}})+(1-x)\Delta_{d,j}(\mathrm{Li^+})+(1-x)\Delta_{d,j}(M^{3+})+2(1-x)\Delta_{d,j}(\mathrm{O^{2-}})\end{aligned} \quad (19)$$

When M is $\mathrm{Ni_{1/2}Mn_{1/2}}$, the mathematical models for estimating the $\Delta H^{\theta}_{f,298}$, $\Delta G^{\theta}_{f,298}$, and C_p of lithium-rich

manganese-based $x\mathrm{Li[Li_{1/3}Mn_{2/3}]O_2}\cdot(1-x)\mathrm{Li}M\mathrm{O_2}$ solid solution materials by the group contribution method are shown in Eq.(20~22):

$$\Delta H^{\theta}_{\mathrm{f},298}(x\mathrm{Li[Li_{1/3}Mn_{2/3}]O_2}\cdot(1-x)\mathrm{LiNi_{1/2}Mn_{1/2}O_2}) = -66.262x-728.847 \quad (20)$$

$$\Delta G^{\theta}_{\mathrm{f},298}(x\mathrm{Li[Li_{1/3}Mn_{2/3}]O_2}\cdot(1-x)\mathrm{LiNi_{1/2}Mn_{1/2}O_2}) = -72.500x-676.458 \quad (21)$$

$$C_{\mathrm{p}}(x\mathrm{Li[Li_{1/3}Mn_{2/3}]O_2}\cdot(1-x)\mathrm{LiNi_{1/2}Mn_{1/2}O_2}) = -6.634x+81.395+(8.385x+35.899)(10^{-3})T+(0.116x-1.191)(10^{6})/T^{2}+(0.415x+5.666)(10^{-6})T^{2} \quad (22)$$

When M is $\mathrm{Ni_{1/3}Co_{1/3}Mn_{1/3}}$, the mathematical models for estimating the $\Delta H^{\theta}_{\mathrm{f},298}$, $\Delta G^{\theta}_{\mathrm{f},298}$, and C_{p} of lithium-rich manganese-based $x\mathrm{Li[Li_{1/3}Mn_{2/3}]O_2}\cdot(1-x)\mathrm{Li}M\mathrm{O_2}$ solid solution materials by the group contribution method are shown in Eq.(23~25):

$$\Delta H^{\theta}_{\mathrm{f},298}(x\mathrm{Li[Li_{1/3}Mn_{2/3}]O_2}\cdot(1-x)\mathrm{LiNi_{1/3}Co_{1/3}Mn_{1/3}O_2}) = -83.145x-711.964 \quad (23)$$

$$\Delta G^{\theta}_{\mathrm{f},298}(x\mathrm{Li[Li_{1/3}Mn_{2/3}]O_2}\cdot(1-x)\mathrm{LiNi_{1/3}Co_{1/3}Mn_{1/3}O_2}) = -92.952x-656.005 \quad (24)$$

$$C_{\mathrm{p}}(x\mathrm{Li[Li_{1/3}Mn_{2/3}]O_2}\cdot(1-x)\mathrm{LiNi_{1/3}Co_{1/3}Mn_{1/3}O_2}) = -14.869x+89.630+(24.973x+19.311)(10^{-3})T+(0.269x-1.344)(10^{6})/T^{2}+(3.866x+2.215)(10^{-6})T^{2} \quad (25)$$

2.3 Mathematical models for estimating $\Delta H^{\theta}_{\mathrm{f},298}$, $\Delta G^{\theta}_{\mathrm{f},298}$, and C_{p} of the layered spinel composite solid solution material

The chemical valences of Li, O in layered spinel $x\mathrm{Li[Li_{1/3}Mn_{2/3}]O_2}\cdot(1-x)\mathrm{LiMn_2O_4}$ ($0<x<1$) composite solid solution material are +1, −2, respectively. The Mn element present in $\mathrm{Li[Li_{1/3}Mn_{2/3}]O_2}$ has a valence of +4, and $\mathrm{LiMn_2O_4}$ has a $\mathrm{Mn^{3+}}$ and $\mathrm{Mn^{4+}}$ content of 50%.

The mathematical models for estimating the $\Delta H^{\theta}_{\mathrm{f},298}$, $\Delta G^{\theta}_{\mathrm{f},298}$, and C_{p} of the layered spinel $x\mathrm{Li[Li_{1/3}Mn_{2/3}]O_2}\cdot(1-x)\mathrm{LiMn_2O_4}$ composite solid solution materials using the group contribution method are shown in Eq.(26~28), respectively:

$$\Delta H^{\theta}_{\mathrm{f},298}(x\mathrm{Li[Li_{1/3}Mn_{2/3}]O_2}\cdot(1-x)\mathrm{LiMn_2O_4}) = 4/3x\Delta H^{\theta}_{\mathrm{f},298}(\mathrm{Li^{+}})+2/3x\Delta H^{\theta}_{\mathrm{f},298}(\mathrm{Mn^{4+}})+2x\Delta H^{\theta}_{\mathrm{f},298}(\mathrm{O^{2-}})+(1-x)\Delta H^{\theta}_{\mathrm{f},298}(\mathrm{Li^{+}})+2\times0.5(1-x)\Delta H^{\theta}_{\mathrm{f},298}(\mathrm{Mn^{3+}})+2\times0.5(1-x)\Delta H^{\theta}_{\mathrm{f},298}(\mathrm{Mn^{4+}})+4(1-x)\Delta H^{\theta}_{\mathrm{f},298}(\mathrm{O^{2-}}) \quad (26)$$

$$\Delta G^{\theta}_{\mathrm{f},298}(x\mathrm{Li[Li_{1/3}Mn_{2/3}]O_2}\cdot(1-x)\mathrm{LiMn_2O_4}) = 4/3x\Delta G^{\theta}_{\mathrm{f},298}(\mathrm{Li^{+}})+2/3x\Delta G^{\theta}_{\mathrm{f},298}(\mathrm{Mn^{4+}})+2x\Delta G^{\theta}_{\mathrm{f},298}(\mathrm{O^{2-}})+(1-x)\Delta G^{\theta}_{\mathrm{f},298}(\mathrm{Li^{+}})+2\times0.5(1-x)\Delta G^{\theta}_{\mathrm{f},298}(\mathrm{Mn^{3+}})+2\times0.5(1-x)\Delta G^{\theta}_{\mathrm{f},298}(\mathrm{Mn^{4+}})+4(1-x)\Delta G^{\theta}_{\mathrm{f},298}(\mathrm{O^{2-}}) \quad (27)$$

$$C_{\mathrm{p}}(x\mathrm{Li[Li_{1/3}Mn_{2/3}]O_2}\cdot(1-x)\mathrm{LiMn_2O_4}) = \sum_j n_j\Delta_{\mathrm{a},j}+(\sum_j n_j\Delta_{\mathrm{b},j}\times10^{-3})T+(\sum_j n_j\Delta_{\mathrm{c},j}\times10^{6})/T^{2}+(\sum_j n_j\Delta_{\mathrm{d},j}\times10^{-6})T^{2}$$

$$\sum_j n_j\Delta_{\mathrm{a},j} = 4/3x\Delta_{\mathrm{a},j}(\mathrm{Li^{+}})+2/3x\Delta_{\mathrm{a},j}(\mathrm{Mn^{4+}})+2x\Delta_{\mathrm{a},j}(\mathrm{O^{2-}})+(1-x)\Delta_{\mathrm{a},j}(\mathrm{Li^{+}})+2\times0.5(1-x)\Delta_{\mathrm{a},j}(\mathrm{Mn^{3+}})+2\times0.5(1-x)\Delta_{\mathrm{a},j}(\mathrm{Mn^{4+}})+4(1-x)\Delta_{\mathrm{a},j}(\mathrm{O^{2-}})$$

$$\sum_j n_j\Delta_{\mathrm{b},j} = 4/3x\Delta_{\mathrm{b},j}(\mathrm{Li^{+}})+2/3x\Delta_{\mathrm{b},j}(\mathrm{Mn^{4+}})+2x\Delta_{\mathrm{b},j}(\mathrm{O^{2-}})+(1-x)\Delta_{\mathrm{b},j}(\mathrm{Li^{+}})+2\times0.5(1-x)\Delta_{\mathrm{b},j}(\mathrm{Mn^{3+}})+2\times0.5(1-x)\Delta_{\mathrm{b},j}(\mathrm{Mn^{4+}})+4(1-x)\Delta_{\mathrm{b},j}(\mathrm{O^{2-}})$$

$$\sum_j n_j\Delta_{\mathrm{c},j} = 4/3x\Delta_{\mathrm{c},j}(\mathrm{Li^{+}})+2/3x\Delta_{\mathrm{c},j}(\mathrm{Mn^{4+}})+2x\Delta_{\mathrm{c},j}(\mathrm{O^{2-}})+(1-x)\Delta_{\mathrm{c},j}(\mathrm{Li^{+}})+2\times0.5(1-x)\Delta_{\mathrm{c},j}(\mathrm{Mn^{3+}})+2\times0.5(1-x)\Delta_{\mathrm{c},j}(\mathrm{Mn^{4+}})+4(1-x)\Delta_{\mathrm{c},j}(\mathrm{O^{2-}})$$

$$\sum_j n_j\Delta_{\mathrm{d},j} = 4/3x\Delta_{\mathrm{d},j}(\mathrm{Li^{+}})+2/3x\Delta_{\mathrm{d},j}(\mathrm{Mn^{4+}})+2x\Delta_{\mathrm{d},j}(\mathrm{O^{2-}})+(1-x)\Delta_{\mathrm{d},j}(\mathrm{Li^{+}})+2\times0.5(1-x)\Delta_{\mathrm{d},j}(\mathrm{Mn^{3+}})+2\times0.5(1-x)\Delta_{\mathrm{d},j}(\mathrm{Mn^{4+}})+4(1-x)\Delta_{\mathrm{d},j}(\mathrm{O^{2-}}) \quad (28)$$

In Eq. (28), the values of the group contribution can be considered as the contributions in the layered spinel $x\mathrm{Li[Li_{1/3}Mn_{2/3}]O_2}\cdot(1-x)\mathrm{LiMn_2O_4}$ composite solid solution material. The mathematical models of $\Delta H^{\theta}_{\mathrm{f},298}$, $\Delta G^{\theta}_{\mathrm{f},298}$, and C_{p} are shown in Eq.(29~31), respectively:

$$\Delta H^{\theta}_{\mathrm{f},298}(x\mathrm{Li[Li_{1/3}Mn_{2/3}]O_2}\cdot(1-x)\mathrm{LiMn_2O_4}) = 446.175x-1241.284 \quad (29)$$

$$\Delta G^{\theta}_{\mathrm{f},298}(x\mathrm{Li[Li_{1/3}Mn_{2/3}]O_2}\cdot(1-x)\mathrm{LiMn_2O_4}) = 454.248x-1203.205 \quad (30)$$

$$C_{\mathrm{p}}(x\mathrm{Li[Li_{1/3}Mn_{2/3}]O_2}\cdot(1-x)\mathrm{LiMn_2O_4}) = -58.806x+133.567+(-33.131x+77.414)(10^{-3})T+(0.823x-1.898)(10^{6})/T^{2}+(3.508x+2.573)(10^{-6})T^{2} \quad (31)$$

In the layered spinel $x\mathrm{Li[Li_{1/3}Mn_{2/3}]O_2}\cdot(1-x)\mathrm{LiNi_{0.5}Mn_{1.5}O_4}$ ($0<x<1$) composite solid solution material, the chemical valences of Li and O are +1 and −2, respectively. The mathematical models for estimating the $\Delta H^{\theta}_{\mathrm{f},298}$, $\Delta G^{\theta}_{\mathrm{f},298}$, and C_{p} of the layered spinel $x\mathrm{Li[Li_{1/3}Mn_{2/3}]O_2}\cdot(1-x)\mathrm{LiNi_{0.5}Mn_{1.5}O_4}$ composite solid solution materials using the group contribution method are shown in Eq.(32~34), respectively:

$$\Delta H^{\theta}_{\mathrm{f},298}(x\mathrm{Li[Li_{1/3}Mn_{2/3}]O_2}\cdot(1-x)\mathrm{LiNi_{0.5}Mn_{1.5}O_4}) = 4/3x\Delta H^{\theta}_{\mathrm{f},298}(\mathrm{Li^{+}})+2/3x\Delta H^{\theta}_{\mathrm{f},298}(\mathrm{Mn^{4+}})+2x\Delta H^{\theta}_{\mathrm{f},298}(\mathrm{O^{2-}})+(1-x)\Delta H^{\theta}_{\mathrm{f},298}(\mathrm{Li^{+}})+0.5(1-x)\Delta H^{\theta}_{\mathrm{f},298}(\mathrm{Ni^{2+}})+1.5(1-x)\Delta H^{\theta}_{\mathrm{f},298}(\mathrm{Mn^{4+}})4(1-x)\Delta H^{\theta}_{\mathrm{f},298}(\mathrm{O^{2-}}) \quad (32)$$

$$\Delta G^{\theta}_{\mathrm{f},298}(x\mathrm{Li[Li_{1/3}Mn_{2/3}]O_2}\cdot(1-x)\mathrm{LiNi_{0.5}Mn_{1.5}O_4}) = 4/3x\Delta G^{\theta}_{\mathrm{f},298}(\mathrm{Li^{+}})+2/3x\Delta G^{\theta}_{\mathrm{f},298}(\mathrm{Mn^{4+}})+2x\Delta G^{\theta}_{\mathrm{f},298}(\mathrm{O^{2-}})+(1-x)\Delta G^{\theta}_{\mathrm{f},298}(\mathrm{Li^{+}})+0.5(1-x)\Delta G^{\theta}_{\mathrm{f},298}(\mathrm{Ni^{2+}})+1.5(1-x)\Delta G^{\theta}_{\mathrm{f},298}(\mathrm{Mn^{4+}})+4\ (1-x)\Delta G^{\theta}_{\mathrm{f},298}(\mathrm{O^{2-}}) \quad (33)$$

$$C_{\mathrm{p}}(x\mathrm{Li[Li_{1/3}Mn_{2/3}]O_2}\cdot(1-x)\mathrm{LiNi_{0.5}Mn_{1.5}O_4}) = \sum_j n_j\Delta_{\mathrm{a},j}+(\sum_j n_j\Delta_{\mathrm{b},j}\times10^{-3})T+(\sum_j n_j\Delta_{\mathrm{c},j}\times10^{6})/T^{2}+(\sum_j n_j\Delta_{\mathrm{d},j}\times10^{-6})T^{2} \quad (34)$$

$$\sum_j n_j\Delta_{\mathrm{a},j} = 4/3x\Delta_{\mathrm{a},j}(\mathrm{Li^{+}})+2/3x\Delta_{\mathrm{a},j}(\mathrm{Mn^{4+}})+2x\Delta_{\mathrm{a},j}(\mathrm{O^{2-}})+(1-x)\Delta_{\mathrm{a},j}(\mathrm{Li^{+}})+0.5(1-x)\Delta_{\mathrm{a},j}\mathrm{Ni^{2+}})+1.5(1-x)\Delta_{\mathrm{a},j}(\mathrm{Mn^{4+}})+4\ (1-x)\Delta_{\mathrm{a},j}(\mathrm{O^{2-}})$$

$$\sum_j n_j\Delta_{\mathrm{b},j} = 4/3x\Delta_{\mathrm{b},j}(\mathrm{Li^{+}})+2/3x\Delta_{\mathrm{b},j}(\mathrm{Mn^{4+}})+2x\Delta_{\mathrm{b},j}(\mathrm{O^{2-}})+(1-x)\Delta_{\mathrm{b},j}(\mathrm{Li^{+}})+0.5(1-x)\Delta_{\mathrm{b},j}(\mathrm{Ni^{2+}})+1.5(1-x)\Delta_{\mathrm{b},j}(\mathrm{Mn^{4+}})+4(1-x)\Delta_{\mathrm{b},j}(\mathrm{O^{2-}})$$

$$\sum_j n_j\Delta_{\mathrm{c},j} = 4/3x\Delta_{\mathrm{c},j}(\mathrm{Li^{+}})+2/3x\Delta_{\mathrm{c},j}(\mathrm{Mn^{4+}})+2x\Delta_{\mathrm{c},j}(\mathrm{O^{2-}})+(1-x)\Delta_{\mathrm{c},j}(\mathrm{Li^{+}})+0.5(1-x)\Delta_{\mathrm{c},j}(\mathrm{Ni^{2+}})+1.5(1-x)\Delta_{\mathrm{c},j}(\mathrm{Mn^{4+}})+4(1-x)\Delta_{\mathrm{c},j}(\mathrm{O^{2-}})$$

$$\sum_j n_j\Delta_{\mathrm{d},j} = 4/3x\Delta_{\mathrm{d},j}(\mathrm{Li^{+}})+2/3x\Delta_{\mathrm{d},j}(\mathrm{Mn^{4+}})+2x\Delta_{\mathrm{d},j}(\mathrm{O^{2-}})+(1-x)\Delta_{\mathrm{d},j}(\mathrm{Li^{+}})+0.5(1-x)\Delta_{\mathrm{d},j}(\mathrm{Ni^{2+}})+1.5(1-x)\Delta_{\mathrm{d},j}(\mathrm{Mn^{4+}})+4(1-x)\Delta_{\mathrm{d},j}(\mathrm{O^{2-}})$$

In Eq. (34), the values of the group contribution can be obtained as the layered spinel $x\mathrm{Li[Li_{1/3}Mn_{2/3}]O_2}\cdot(1-x)\mathrm{LiNi_{0.5}Mn_{1.5}O_4}$ composite solid solution material. The mathematical models of $\Delta H^{\theta}_{\mathrm{f},298}$, $\Delta G^{\theta}_{\mathrm{f},298}$, and C_{p} are shown in Eq.(35~37), respectively:

$$\Delta H^{\theta}_{\mathrm{f},298}(x\mathrm{Li[Li_{1/3}Mn_{2/3}]O_2}\cdot(1-x)\mathrm{LiNi_{0.5}Mn_{1.5}O_4}) = 366.851x-1161.960 \quad (35)$$

$$\Delta G^{\theta}_{\mathrm{f},298}(x\mathrm{Li[Li_{1/3}Mn_{2/3}]O_2}\cdot(1-x)\mathrm{LiNi_{0.5}Mn_{1.5}O_4}) = 320.593x-1069.550 \quad (36)$$

$$C_p(xLi[Li_{1/3}Mn_{2/3}]O_2\cdot(1-x)LiNi_{0.5}Mn_{1.5}O_4)=-59.345x+134.106+(-37.749x+82.033)(10^{-3})T+(0.967x-2.042)(10^6)/T^2+(3.217x+2.864)(10^{-6})T^2 \quad (37)$$

The $\Delta H^{\theta}_{f,298}$, $\Delta G^{\theta}_{f,298}$, and C_p of the common 63 lithium-rich materials were estimated by the mathematical models, as show in Table 7.

Table 7 Estimation results of $\Delta H^{\theta}_{f,298}$, $\Delta G^{\theta}_{f,298}$ and $C_{p,298}$ for lithium-rich materials

Sample	$\Delta H^{\theta}_{f,298}$/kJ·mol^{-1}	$\Delta G^{\theta}_{f,298}$/kJ·mol^{-1}	$C_{p,298}$ predicted by the group contribution method/ J·mol^{-1}·K^{-1}	$C_{p,298}$ predicted by the Kopp's rule/ J·mol^{-1}·K^{-1}
$0.1Li_2MnO_3\cdot0.9LiCoO_2$	−729.65	−665.93	86.13	79.70
$0.2Li_2MnO_3\cdot0.8LiCoO_2$	−781.09	−716.77	89.30	83.60
$0.3Li_2MnO_3\cdot0.7LiCoO_2$	−832.54	−767.60	92.46	87.51
$0.4Li_2MnO_3\cdot0.6LiCoO_2$	−883.99	−818.43	95.62	91.41
$0.5Li_2MnO_3\cdot0.5LiCoO_2$	−935.43	−869.27	98.78	95.31
$0.6Li_2MnO_3\cdot0.4LiCoO_2$	−986.88	−920.10	101.95	99.21
$0.7Li_2MnO_3\cdot0.3LiCoO_2$	−1038.32	−970.94	105.11	103.11
$0.8Li_2MnO_3\cdot0.2LiCoO_2$	−1089.77	−1021.77	108.27	107.02
$0.9Li_2MnO_3\cdot0.1LiCoO_2$	−1141.22	−1072.60	111.43	110.92
$0.1Li_2MnO_3\cdot0.9LiFeO_2$	−806.02	−759.05	85.64	82.74
$0.2Li_2MnO_3\cdot0.8LiFeO_2$	−848.98	−799.54	88.85	86.30
$0.3Li_2MnO_3\cdot0.7LiFeO_2$	−891.94	−840.03	92.07	89.87
$0.4Li_2MnO_3\cdot0.6LiFeO_2$	−934.90	−880.51	95.29	93.43
$0.5Li_2MnO_3\cdot0.5LiFeO_2$	−977.86	−921.00	98.51	97.00
$0.6Li_2MnO_3\cdot0.4LiFeO_2$	−1020.82	−961.49	101.72	100.56
$0.7Li_2MnO_3\cdot0.3LiFeO_2$	−1063.78	−1001.97	104.94	104.13
$0.8Li_2MnO_3\cdot0.2LiFeO_2$	−1106.74	−1042.46	108.16	107.69
$0.9Li_2MnO_3\cdot0.1LiFeO_2$	−1149.70	−1082.95	111.38	111.26
$0.1Li_2MnO_3\cdot0.9LiNi_{1/2}Mn_{1/2}O_2$	−775.23	−721.16	82.73	80.65
$0.2Li_2MnO_3\cdot0.8LiNi_{1/2}Mn_{1/2}O_2$	−821.61	−765.85	86.27	84.44
$0.3Li_2MnO_3\cdot0.7LiNi_{1/2}Mn_{1/2}O_2$	−867.99	−810.55	89.80	88.24
$0.4Li_2MnO_3\cdot0.6LiNi_{1/2}Mn_{1/2}O_2$	−914.37	−855.25	93.34	92.04
$0.5Li_2MnO_3\cdot0.5LiNi_{1/2}Mn_{1/2}O_2$	−960.76	−899.95	96.88	95.84
$0.6Li_2MnO_3\cdot0.4LiNi_{1/2}Mn_{1/2}O_2$	−1007.14	−944.65	100.42	99.63
$0.7Li_2MnO_3\cdot0.3LiNi_{1/2}Mn_{1/2}O_2$	−1053.52	−989.34	103.96	103.43
$0.8Li_2MnO_3\cdot0.2LiNi_{1/2}Mn_{1/2}O_2$	−1099.90	−1034.04	107.50	107.23
$0.9Li_2MnO_3\cdot0.1LiNi_{1/2}Mn_{1/2}O_2$	−1146.28	−1078.74	111.04	111.02
$0.1Li[Li_{1/3}Mn_{2/3}]O_2\cdot0.9LiNi_{1/2}Mn_{1/2}O_2$	−735.47	−683.71	78.91	76.82
$0.2Li[Li_{1/3}Mn_{2/3}]O_2\cdot0.8LiNi_{1/2}Mn_{1/2}O_2$	−742.10	−690.96	78.63	76.79
$0.3Li[Li_{1/3}Mn_{2/3}]O_2\cdot0.7LiNi_{1/2}Mn_{1/2}O_2$	−748.73	−698.21	78.35	76.76
$0.4Li[Li_{1/3}Mn_{2/3}]O_2\cdot0.6LiNi_{1/2}Mn_{1/2}O_2$	−755.35	−705.46	78.07	76.73
$0.5Li[Li_{1/3}Mn_{2/3}]O_2\cdot0.5LiNi_{1/2}Mn_{1/2}O_2$	−761.98	−712.71	77.79	76.70
$0.6Li[Li_{1/3}Mn_{2/3}]O_2\cdot0.4LiNi_{1/2}Mn_{1/2}O_2$	−768.60	−719.96	77.51	76.67
$0.7Li[Li_{1/3}Mn_{2/3}]O_2\cdot0.3LiNi_{1/2}Mn_{1/2}O_2$	−775.23	−727.21	77.23	76.64
$0.8Li[Li_{1/3}Mn_{2/3}]O_2\cdot0.2LiNi_{1/2}Mn_{1/2}O_2$	−781.86	−734.46	76.95	76.61
$0.9Li[Li_{1/3}Mn_{2/3}]O_2\cdot0.1LiNi_{1/2}Mn_{1/2}O_2$	−788.48	−741.71	76.67	76.58
$0.1Li[Li_{1/3}Mn_{2/3}]O_2\cdot0.9LiNi_{1/3}Co_{1/3}Mn_{1/3}O_2$	−720.28	−665.30	80.04	76.50
$0.2Li[Li_{1/3}Mn_{2/3}]O_2\cdot0.8LiNi_{1/3}Co_{1/3}Mn_{1/3}O_2$	−728.59	−674.60	79.64	76.49
$0.3Li[Li_{1/3}Mn_{2/3}]O_2\cdot0.7LiNi_{1/3}Co_{1/3}Mn_{1/3}O_2$	−736.91	−683.89	79.23	76.49
$0.4Li[Li_{1/3}Mn_{2/3}]O_2\cdot0.6LiNi_{1/3}Co_{1/3}Mn_{1/3}O_2$	−745.22	−693.19	78.83	76.48
$0.5Li[Li_{1/3}Mn_{2/3}]O_2\cdot0.5LiNi_{1/3}Co_{1/3}Mn_{1/3}O_2$	−753.54	−702.48	78.42	76.48
$0.6Li[Li_{1/3}Mn_{2/3}]O_2\cdot0.4LiNi_{1/3}Co_{1/3}Mn_{1/3}O_2$	−761.85	−711.78	78.01	76.47

Continued Table 7

Sample	$\Delta H^{\theta}_{f,298}$/kJ·mol^{-1}	$\Delta G^{\theta}_{f,298}$/kJ·mol^{-1}	$C_{p,298}$ predicted by the group contribution method/ J·mol^{-1}·K^{-1}	$C_{p,298}$ predicted by the Kopp's rule/ J·mol^{-1}·K^{-1}
$0.7Li[Li_{1/3}Mn_{2/3}]O_2·0.3LiNi_{1/3}Co_{1/3}Mn_{1/3}O_2$	−770.17	−721.07	77.61	76.47
$0.8Li[Li_{1/3}Mn_{2/3}]O_2·0.2LiNi_{1/3}Co_{1/3}Mn_{1/3}O_2$	−778.48	−730.37	77.20	76.46
$0.9Li[Li_{1/3}Mn_{2/3}]O_2·0.1LiNi_{1/3}Co_{1/3}Mn_{1/3}O_2$	−786.79	−739.66	76.80	76.46
$0.1Li[Li_{1/3}Mn_{2/3}]O_2·0.9LiMn_2O_4$	−1196.67	−1157.78	129.58	127.40
$0.2Li[Li_{1/3}Mn_{2/3}]O_2·0.8LiMn_2O_4$	−1152.05	−1112.36	123.67	121.75
$0.3Li[Li_{1/3}Mn_{2/3}]O_2·0.7LiMn_2O_4$	−1107.43	−1066.93	117.76	116.10
$0.4Li[Li_{1/3}Mn_{2/3}]O_2·0.6LiMn_2O_4$	−1062.81	−1021.51	111.85	110.45
$0.5Li[Li_{1/3}Mn_{2/3}]O_2·0.5LiMn_2O_4$	−1018.20	−976.08	105.94	104.80
$0.6Li[Li_{1/3}Mn_{2/3}]O_2·0.4LiMn_2O_4$	−973.58	−930.66	100.03	99.15
$0.7Li[Li_{1/3}Mn_{2/3}]O_2·0.3LiMn_2O_4$	−928.96	−885.23	94.12	93.50
$0.8Li[Li_{1/3}Mn_{2/3}]O_2·0.2LiMn_2O_4$	−884.34	−839.81	88.21	87.85
$0.9Li[Li_{1/3}Mn_{2/3}]O_2·0.1LiMn_2O_4$	−839.73	−794.38	82.30	82.20
$0.1Li[Li_{1/3}Mn_{2/3}]O_2·0.9LiNi_{0.5}Mn_{1.5}O_4$	−1125.27	−1037.49	129.87	126.23
$0.2Li[Li_{1/3}Mn_{2/3}]O_2·0.8LiNi_{0.5}Mn_{1.5}O_4$	−1088.59	−1005.43	123.93	120.71
$0.3Li[Li_{1/3}Mn_{2/3}]O_2·0.7LiNi_{0.5}Mn_{1.5}O_4$	−1051.90	−973.37	117.99	115.19
$0.4Li[Li_{1/3}Mn_{2/3}]O_2·0.6LiNi_{0.5}Mn_{1.5}O_4$	−1015.22	−941.31	112.04	109.67
$0.5Li[Li_{1/3}Mn_{2/3}]O_2·0.5LiNi_{0.5}Mn_{1.5}O_4$	−978.53	−909.25	106.10	104.15
$0.6Li[Li_{1/3}Mn_{2/3}]O_2·0.4LiNi_{0.5}Mn_{1.5}O_4$	−941.85	−877.19	100.16	98.63
$0.7Li[Li_{1/3}Mn_{2/3}]O_2·0.3LiNi_{0.5}Mn_{1.5}O_4$	−905.16	−845.13	94.22	93.11
$0.8Li[Li_{1/3}Mn_{2/3}]O_2·0.2LiNi_{0.5}Mn_{1.5}O_4$	−868.48	−813.08	88.28	87.59
$0.9Li[Li_{1/3}Mn_{2/3}]O_2·0.1LiNi_{0.5}Mn_{1.5}O_4$	−831.79	−781.02	82.34	82.07

3 Conclusions

1) The $\Delta H^{\theta}_{f,298}$, $\Delta G^{\theta}_{f,298}$, and $C_{p,298}$ of the three types of lithium-rich cathode materials consist of the thermodynamic group contribution values of Li^+, Ni^{2+}, Fe^{3+}, Co^{2+}, Co^{3+}, Mn^{3+}, and Mn^{4+}. Three main types of lithium-rich cathode materials are explored: (1) lithium-rich layered $xLi_2MnO_3·(1-x)LiMO_2$ ($0<x<1$, M=Ni, Co, Cr, Fe, Al, Mg, Ni-Co, Ni-Mn, Ni-Co-Mn…) cathode material, (2) lithium-rich manganese-based $xLi_{1/3}MnO_{2/3}·(1-x)LiMO_2$ ($0<x<1$, M=Ni, Co, Cr, Fe, Al, Mg, Ni-Co, Ni-Mn, Ni-Co-Mn…) solid solution material, and (3) layered spinel $xLi[Li_{1/3}Mn_{2/3}]O_2·(1-x)LiMn_2O_4$ ($0<x<1$) composite solid solution material and layered spinel $xLi[Li_{1/3}Mn_{2/3}]O_2·(1-x)LiNi_{0.5}Mn_{1.5}O_4$ ($0<x<1$) composite solid solution material.

2) The mathematical models for estimating the $\Delta H^{\theta}_{f,298}$, $\Delta G^{\theta}_{f,298}$, and C_p of three types of lithium-rich cathode materials are constructed for the first time by the group contribution method.

3) Based on the satisfactory results, the $\Delta H^{\theta}_{f,298}$, $\Delta G^{\theta}_{f,298}$, and C_p of three types of lithium-rich $Li_{1+x}M_{1-x}O_2$ cathode materials are calculated, and those of 63 common lithium-rich $Li_{1+x}M_{1-x}O_2$ materials can also be estimated by the mathematical models.

References

1 Han Chen, Cao Wenqiang, Cao Maosheng. *Inorg Chem Front*[J], 2020, 21(7): 4101

2 Cao Maosheng, Wang Xixi, Cao Wenqiang *et al. Small*[J], 2018, 14(29): 1 800 987

3 Cao Wenqiang, Wang Wenzhong, Shi Honglong *et al. Nano Res* [J], 2018, 11(3): 1437

4 Cao Maosheng, Wang Xixi, Zhang Min *et al. Adv Funct Mater* [J], 2019, 29(25): 1 807 398

5 Hassoun J, Lee K S, Sun Y K *et al. Journal of the American Chemical Society*[J], 2011, 133(9): 3139

6 Li Hong. *Energy Storage Science and Technology*[J], 2015, 4(3): 306 (in Chinese)

7 Etacheri V, Marom R, Elazari R *et al. Energy Environ Sci*[J], 2011, 4(9): 3243

8 Thackeray M M, Kang S H, Johnson C S *et al. Journal of Materials Chemistry*[J], 2007, 17(30): 3112

9 Zhang Lianqi, Ren Libin, Liu Xingjiang *et al. Chinese Journal of Power Sources*[J], 2009, 33(5): 426 (in Chinese)

10 Yao Lihua, Cao Wenqiang, Cao Maosheng *et al. Chemical Engineering Journal*[J], 2021, 413: 127 428

11 Lu Z, Beaulieu L Y, Donaberger R A *et al. Journal of the Electrochemical Society*[J], 2002, 149(6): 778

12 Boulineau A, Croguennec L, Delmas C *et al. Chemistry of Materials*[J], 2009, 21(18): 4216

13 Armstrong A R, Holzapfel M, Novák P *et al. Journal of the American Chemical Society*[J], 2006, 128(26): 8694

14 Kim J S, Johnson C S, Vaughey J T *et al. Chemistry of Materials* [J], 2004, 16(10): 1996

15 Kang S H, Amine K. *Journal of Power Sources*[J], 2005, 146(1): 654

16 Wei X, Zhang S, Du Z *et al. Electrochimica Acta*[J], 2013, 107: 549

17 Shi S J, Tu J P, Tang Y Y *et al*. *Journal of Power Sources*[J], 2013, 228: 14

18 Peng Qingwen, Liu Xingjiang. *Chinese Journal of Power Sources*[J], 2017(9): 1248 (in Chinese)

19 Wang Zhao, Wu Feng, Su Yuefeng *et al. Acta Physico-Chimica Sinica*[J], 2012, 28(4): 823

20 He Wei, Qian Jiangfeng, Cao Yuliang *et al. RSC Advances*[J], 2012, 2(8): 3423

21 Jarvis K A, Deng Z, Allard L F *et al. Chemistry of Materials*[J], 2011, 23(16): 3614

22 Lee D K, Park S H, Amine K *et al. Journal of Power Sources*[J], 2006, 162(2): 1346

23 Kim J H, Park C W, Sun Y K. *Solid State Ionics*[J], 2003, 164(1): 43

24 Arunkumar T A, Wu Y, Manthiram A. *Chemistry of Materials*[J], 2007, 19(12): 3067

25 Wang Q Y, Liu J, Murugan A V *et al*. *Journal of Materials Chemistry*[J], 2009, 19(28): 4965

26 Yabuuchi N, Yoshii K, Myung S T *et al. Journal of the American Chemical Society*[J], 2011, 133(12): 4404

27 Mostafa A T M G, Eakman J M, Yarbro S L. *Guizhou Chemical Industry*[J], 1997, 34(12): 4577 (in Chinese)

28 Mostafa A T M G, Eakman J M, Montoya M M *et al. Industrial & Engineering Chemistry Research*[J],1996, 35(1): 343

29 Dean J A. *Lange's Handbook of Chemistry*[M]. Beijing: Science Press, 2003: 977

30 Leitner J, Chuchvalec P, Sedmidubsky D *et al. Thermochimica Acta*[J], 2002, 395(1): 27

31 Yang Lixin, Wang Dahui, Chen Huaijing *et al. Rare Metal Materials and Engineering*[J], 2020, 49(1): 161 (in Chinese)

32 Lixin Yang, Dahui Wang, Huaijing Chen *et al. Rare Metals*[J], 2020, 44(10): 1053 (in Chinese)

基于基团贡献法估算(富锂)锂离子电池正极材料$Li_{1+x}M_{1-x}O_2$的热力学性质

王大辉[1]，甘先豪[1]，陈怀敬[2]，杨立新[1]，胡平平[1]，刘振宁[1]

(1. 兰州理工大学 省部共建有色金属先进加工与再利用国家重点实验室，甘肃 兰州 730050)

(2. 兰州理工大学 理学院，甘肃 兰州 730050)

摘　要：富锂$Li_{1+x}M_{1-x}O_2$材料的研究主要集中在其结构和电化学性能上，而很少关注其热力学性能。开发具有高能量密度和容量的新型富锂材料取决于这种材料的结构、热力学性质和电化学性质之间的固有关系。对富锂材料$Li_{1+x}M_{1-x}O_2$的热力学性质了解不足，使得新型$Li_{1+x}M_{1-x}O_2$材料的开发和利用受到限制。鉴于$Li_{1+x}M_{1-x}O_2$材料缺乏热力学数据，根据基团贡献方法的原理对$LiAlO_2$进行拆分。基于热力学原理，提出了用于估计$LiAlO_2$的$\Delta G^{\theta}_{f,298}$、$\Delta H^{\theta}_{f,298}$和$C_p$的数学模型。采用基团贡献法估算了56种固体无机化合物的$\Delta G^{\theta}_{f,298}$和$\Delta H^{\theta}_{f,298}$以及54种固体无机化合物的$C_{p,298}$，以检验该模型的可靠性和适用性。利用基团贡献法估算了固体无机化合物的数学模型。利用基团贡献法拟合的基团参数选择的实验数据准确可靠。在结果令人满意的基础上，建立了用于估算3种类型的$Li_{1+x}M_{1-x}O_2$材料的$\Delta G^{\theta}_{f,298}$，$\Delta H^{\theta}_{f,298}$和$C_p$的数学模型，并估算了63种常见$Li_{1+x}M_{1-x}O_2$材料的$\Delta G^{\theta}_{f,298}$、$\Delta H^{\theta}_{f,298}$和$C_{p,298}$。

关键词：富锂正极材料；基团贡献法；$\Delta G^{\theta}_{f,298}$；$\Delta H^{\theta}_{f,298}$；$C_{p,298}$

作者简介：王大辉，男，1972年生，博士，教授，兰州理工大学材料科学与工程学院，甘肃 兰州 730050，E-mail：wangdh@lut.edu.cn